PONTIFICIA UNIVERSIDAD CATÓLICA DEL PERÚ

ESCUELA DE POSGRADO

Experimental display of the extended polarization coherence theorem

Trabajo de investigación para optar el grado de Magíster en Física que presenta:

AUTOR:

Fabio Joel Auccapuclla Quispe

ASESOR:

Prof. Francisco Antonio De Zela Martinez

JURADO:

Prof. Eduardo Ruben Massoni Kamimoto
Prof. Hernan Alfredo Castillo Egoavil

Lima, 2019

Resumen

En el presente trabajo reportamos los resultados experimentales que muestran la interacción entre visibilidad, distinguibilidad y grado de polarización, estos gobernados por una reciente extensión del teorema polarización y coherencia (PCT). Esta clase de teoremas tratan dualidad en ambos escenarios tanto cuánticos como clásicos. Nosotros particularmente nos enfocamos en el vector inherente natural del grado de libertad de polarización y mostramos varios efectos que van mas allá del alcance original del teorema PCT. Nuestros resultados exhiben características que pueden ser compartidas por fenómenos cuánticos y clásicos, siempre que estos fenómenos reflejen alguna coherencia oculta o expuesta.
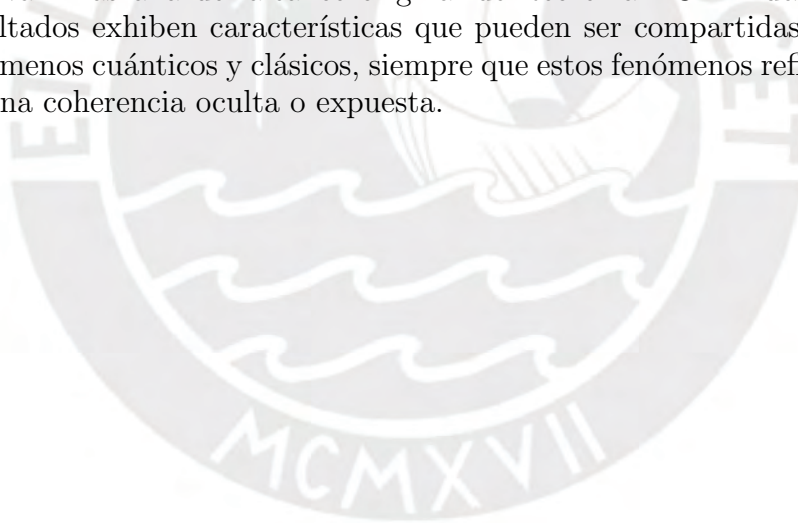
Agradecimientos

Sin lugar a dudas, primero quiero comenzar agradeciendo a mi madre por siempre estar apoyandome en todas las dediciones que he tomado a lo largo de mi vida, basicamente no hubiera podido llegar a este punto de mi vida sin ella. Así mismo, agradecer a mi hermana por ser una amiga incondicional a lo largo de todos estos años.

También agradecer al profesor Francisco de Zela por todo lo enseñado y por el apoyo brindado a lo largo de la maestría. Además, agradecerle por formar el grupo de Óptica Cuántica y siempre tener las puertas abiertas para todo aquel que tenga interés sin importar los conocimientos previos. En este punto, quiero expresar mi profunda gratitud hacia cada uno de los integrantes del grupo. Comenzando por las personas con las cuales realice el presente trabajo: Victor Avalos, Junior Gonzales, Piero Sanchez y Elmer Suarez. Y por ultimo, agradecer a Yonny Yucra por la ayuda brindada mientras realizabamos el experimento.

Finalmente, agradecer a CIENCIACTIVA-CONCYTEC por la ayuda financiera ortogado en forma de beca con la cual ser posible completar este trabajo.

Optics Letters

Experimental display of the extended polarization coherence theorem

P. Sánchez, J. Gonzales, V. Avalos, [ID] **F. Auccapuclla, E. Suarez, and F. De Zela*** [ID]

Departamento de Ciencias, Sección Física, Pontificia Universidad Católica del Perú, Apartado 1761, Lima, Peru
Corresponding author: fdezela@pucp.edu.pe

We report experimental results that show the interplay between visibility, distinguishability, and the degree of polarization, as ruled by a recent extension of the polarization coherence theorem (PCT). Theorems of this kind address duality in both quantum and classical scenarios. We particularly focus on the inherent vector nature of the polarization degree of freedom and display various effects that lie beyond the scope of the original PCT. Our results exhibit features that can be shared by quantum and classical phenomena, whenever these phenomena reflect some hidden or exposed coherence. © 2019 Optical Society of America

Duality and entanglement are perhaps the most prominent hallmarks of quantum mechanics. Both evoke a sense of weirdness which has been however no obstacle for their instrumentation as powerful tools, useful not only for an accurate description of physical phenomena but for many practical applications as well. It is thus important to elucidate the various possible forms in which duality and entanglement manifest themselves. Recent developments have shown that the defining features of duality and entanglement may arise in both the quantum and the classical domain. An important result in this respect is the recently established polarization-coherence-theorem (PCT) [1], which is one of the few quantitative statements about those paradoxical features that have characterized the quantum formulation since its very inception. The PCT has a very simple mathematical structure: $V^2 + D^2 = P^2$. Here, three different measures, visibility (V), distinguishability (D), and the degree of polarization (P), merge into an equality. The two sides of duality, e.g., its wave-like and its particle-like nature, are hereby mutually constrained. The underlying scheme corresponds to a two-path interferometric setup, with respect to which V and D are defined. While V measures the visibility of the interferometric pattern, D measures the distinguishability of one path over the other. The third party, the degree of polarization P, is the required marker of one or the other path. Concurrence (C), a standard measure of entanglement, has recently—and quite unexpectedly—entered the scene through its identification by Eberly and coworkers, as a sort of polarization's alter ego [2]. Indeed, these authors have

established the rather surprising relationship: $C^2 + P^2 = 1$, which immediately leads to $V^2 + D^2 + C^2 = 1$, a variant of the PCT in which the two aforementioned quantum hallmarks, duality and entanglement, take part of one and the same constraint [3].

A sort of preamble to the PCT was established years ago and within a strictly quantum context, in the form of an inequality: $V^2 + D^2 \leq 1$ [4–6]. Such a constraint is implied by the PCT, as a consequence of $P^2 \leq 1$. Now, the PCT not only extended the above inequality to a tight equality, it also extended its domain of applicability by embracing both the classical and the quantum context. This should come as no surprise, if we recall that wave-particle duality is nothing but a variant of the wave-ray duality that so much steered the way in which de Broglie and Schrödinger originally developed the quantum formalism. Fermat's principle in classical optics goes hand-in-hand with Hamilton's principle in classical mechanics. The two principles are formulated in terms of paths, e.g., ray-like concepts. While Fermat's principle proved to be a limiting case of Maxwell's wave equation, Schrödinger's equation arose as an attempt to formulate a wave equation whose limiting case should be Hamilton's principle. Even though such a relationship was never established, we may expect manifold manifestations of a latent common ground shared by quantum and classical phenomena. Latest developments in the realm of quantum and classical optics are fully in line with these expectations [7–16].

The two aforementioned variants of the PCT brought to the fore some links between concepts that so far seemed to be unrelated to each other. A case in point is the link joining polarization and concurrence. Their mutual interdependence becomes clear after one realizes that completely polarized states ($P = 1$) are necessarily unentangled ($C = 0$), as it follows from $C^2 + P^2 = 1$. This is in line with the fact that a system in a pure state cannot be entangled with a second one. Likewise, full bipartite entanglement ($C = 1$) requires that each party is in a fully unpolarized state ($P = 0$). Thus, even though polarization is usually defined with reference to a single system, there is a second system—called "environment" or otherwise—that must be considered whenever P deviates from its extremal value $P = 1$. An interferometric setup represents the possibly simplest means to exhibit the interplay between two systems. A binary path can be one system, while an "internal" degree of freedom (DOF), e.g., polarization, may serve as the second

system [17]. The corresponding interferogram can contain much information. In relation to the path-DOF, we have the relative phase-difference as the most obvious one. This is a scalar quantity. On the other hand, polarization has an inherent vectorial nature, as evidenced by the corresponding Stokes vector. By submitting this vector to different transformations, we may manipulate various features, e.g., geometric phases in pure and mixed states [18]. We can also uncover how quantities such as V, D, and P relate to one another when the "marker" DOF is submitted to unitary transformations. This is our main concern here. Our aim is to experimentally exhibit an extension of the PCT [19], in which unitary transformations leave their sign in the recorded interferogram. We can recover the PCT by conveniently choosing the unitary, thereby hiding it from observation. On the contrary, by exposing the unitary, it becomes possible to exhibit additional features of the interplay between the various DOFs that one may access with a given setup.

In what follows, we first present the extension of the PCT. We then discuss our experimental setup, which serves to display different features of the extended PCT. Finally, we report our results and comment on their most salient aspects.

As we said before, visibility and distinguishability are mutually constrained by inequality $V^2 + D^2 \leq 1$, which was originally derived using the quantum formalism [4–6]. The assumed physical framework is a two-arm interferometric setup, supplemented with appropriate devices on each arm to perform some unitary transformations, U_1 and U_2, as shown in Fig. 1. These transformations apply to an "internal" DOF, e.g., electron's spin or photon's polarization. Such an internal DOF can be represented in a two-dimensional Hilbert space and, likewise, the binary path-DOF. We are thus dealing with a two-qubit Hilbert space. We notice that these DOFs have no quantum nature by themselves. They can be equally assigned to both classical and quantum objects, depending on the physical realization. In both cases, the internal DOF serves as a path marker. The more effective this marker is, the more distinguishable is one path from the other and the less visible is the interferogram that can be registered at the output of the arrangement. V and D are thus complementary features, the relative importance of which is mediated by the marker DOF, P in our case.
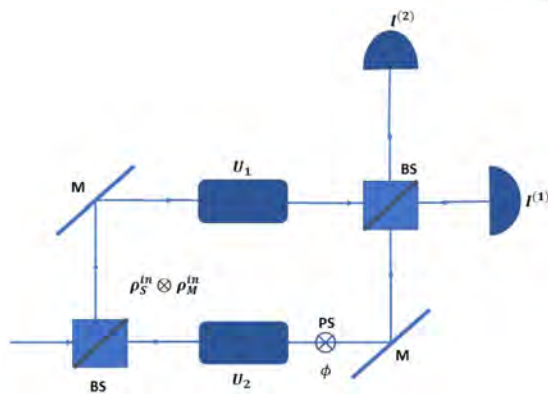

Fig. 1. Mach–Zehnder-type interferometer. A product-state system-marker is submitted to unitaries U_1 and U_2 that act on the marker system alone. BS, beam-splitter; PS, phase shifter.

The above framework served to establish an extension of the PCT [19]. This extension was derived as follows. Let us assume that the system-qubit is in a pure state $|\Psi_S^{\text{in}}\rangle = \alpha|1\rangle + \beta|2\rangle$, and the marker-qubit is in a mixed state

$$\rho_M^{\text{in}} = \frac{1}{2}\left(\sigma_0 + \vec{S}^{\text{in}} \cdot \vec{\sigma}\right). \tag{1}$$

Here, σ_0 is the identity matrix and $\vec{\sigma}$ is the vector of Pauli matrices. $\vec{S}^{\text{in}}$ is the Stokes vector, the norm of which gives the degree of polarization: $P = \left(\vec{S}^{\text{in}} \cdot \vec{S}^{\text{in}}\right)^{1/2}$. Before its submission to the unitaries, the two-qubit system is in the state $\rho_{SM} = \rho_S^{\text{in}} \otimes \rho_M^{\text{in}}$, with $\rho_S^{\text{in}} = |\Psi_S^{\text{in}}\rangle\langle\Psi_S^{\text{in}}|$. The polarization DOF is submitted to different transformations, depending on the arm of the interferometer. Polarization-unitary U_1 acts on one arm and unitary U_2 acts on the other arm. The transformation to which ρ_{SM} is submitted, is thus given by

$$U_{SM} = |1\rangle\langle 1| \otimes U_1 + e^{i\delta}|2\rangle\langle 2| \otimes U_2, \tag{2}$$

where δ is the relative phase-shift between arms. After having been transformed by U_{SM}, the two-qubit system is in state $\rho_{SM} = U_{SM}(\rho_S^{\text{in}} \otimes \rho_M^{\text{in}})U_{SM}^\dagger$. At this point, the path-system is in the state $\rho_S = \text{Tr}_M(\rho_{SM})$. The intensity at one output port of the second beam-splitter (see Fig. 1) is given by

$$I = \frac{1}{2}\{|\alpha|^2 + |\beta|^2 + 2\,\text{Re}[\alpha^*\beta\text{Tr}_M(U_1\rho_M^{\text{in}}U_2^\dagger)e^{i\delta}]\}. \tag{3}$$

In terms of this intensity, we define visibility as

$$V = \frac{I^{\max} - I^{\min}}{I^{\max} + I^{\min}} = |\text{Tr}_M(U_1\rho_M^{\text{in}}U_2^\dagger)| = |\text{Tr}_M(U\rho_M^{\text{in}})|, \tag{4}$$

where we have set $U = U_2^\dagger U_1$, a transformation that can be understood as a relative unitary. Similarly, the marker is in a state

$$\rho_M = \text{Tr}_S(\rho_{SM}) = |\alpha|^2\rho_M^{(1)} + |\beta|^2\rho_M^{(2)}, \tag{5}$$

with $\rho_M^{(k)} = U_k\rho_M^{\text{in}}U_k^\dagger$ $(k = 1, 2)$. Equation (5) shows that ρ_M is given by the weighted sum of $\rho_M^{(1)}$ and $\rho_M^{(2)}$, whereby the relative weights depend on the system-qubit $|\Psi_S^{\text{in}}\rangle = \alpha|1\rangle + \beta|2\rangle$. The inherent distinguishability between the two paths can thus be defined as

$$D = \frac{1}{2}\,\text{Tr}|\rho_M^{(1)} - \rho_M^{(2)}| = \frac{1}{2}\,\text{Tr}|U_1\rho_M^{\text{in}}U_1^\dagger - U_2\rho_M^{\text{in}}U_2^\dagger|$$
$$= \frac{1}{2}|\vec{S}_1^{\text{out}} - \vec{S}_2^{\text{out}}|. \tag{6}$$

In the first line above, we use the definition $|A| = \sqrt{A^\dagger A}$ for any linear operator A and in the second line $\vec{S}_k^{\text{out}}$ denotes the Stokes vector that belongs to $\rho_M^{(k)}$. We can write $\vec{S}_k^{\text{out}} = \mathcal{R}_k\vec{S}^{\text{in}}$, where $\mathcal{R}_k$ is the 3D-rotation that is associated to U_k. Hence, $D = \frac{1}{2}|\mathcal{R}_1\vec{S}^{\text{in}} - \mathcal{R}_2\vec{S}^{\text{in}}| = \frac{1}{2}|\mathcal{R}_2^{-1}\mathcal{R}_1\vec{S}^{\text{in}} - \vec{S}^{\text{in}}|$. Rotation $\mathcal{R}_2^{-1}\mathcal{R}_1$ can be specified by a rotation angle γ and a rotation axis $\hat{n}$. Its associated unitary reads

$$U = U_2^\dagger U_1 = \cos\left(\frac{\gamma}{2}\right)\sigma_0 + i\sin\left(\frac{\gamma}{2}\right)\hat{n} \cdot \vec{\sigma}. \tag{7}$$

Using this parameterization, we calculate

$$D^2 = P^2\sin^2(\phi)\sin^2\left(\frac{\gamma}{2}\right), \tag{8}$$

$$V^2 = \cos^2\left(\frac{\gamma}{2}\right) + P^2 \cos^2(\phi)\sin^2\left(\frac{\gamma}{2}\right), \qquad (9)$$

where ϕ is the angle between $\hat{n}$ and $\vec{S}^{\text{in}}$. From the above expressions we get

$$V^2 + D^2 = \cos^2\left(\frac{\gamma}{2}\right) + P^2 \sin^2\left(\frac{\gamma}{2}\right), \qquad (10)$$

as an extension of the PCT. The latter corresponds to the particular case $\gamma = \pi$. Equations (8)–(10) engage not only visibility, distinguishability, and the degree of polarization, but the relative unitary $U = U_2^{-1} U_1 = \exp(i\gamma\hat{n} \cdot \vec{\sigma}/2)$. In contrast to the relative phase $e^{i(\varphi_1 - \varphi_2)}$ between paths, which is a scalar, U contains a richer, vectorial structure. Thus, by considering U we can uncover several features that remain hidden in the PCT. Indeed, according to the PCT the marker should become ineffective when it is in a fully random state ($P = 0$), because in that case $D = V = 0$ as well. The extended version of the PCT, on the other hand, allows us to see some new features. Equations (8) and (9) show that $P = 0$ implies $D = 0$ and $V^2 = \cos^2(\gamma/2)$, so that the visibility is controlled by U alone. This is a somewhat counterintuitive result, as in this case the unitaries seem to have no polarized system on which to act. However, a look at Eq. (4) makes clear what is going on. When $\rho_M^{\text{in}} = \sigma_0/2$, the visibility is given by $V = |\text{Tr}_M U|/2 = |\text{Tr}_M[\cos(\gamma/2)\sigma_0 + i\sin(\gamma/2)\hat{n} \cdot \vec{\sigma}]|/2 = |\cos(\gamma/2)|$. That is, U can leave its imprint on the fully unpolarized part of the state. So, even though a fully random marker-system becomes useless for distinguishing one path from the other ($D = 0$), it remains useful for driving visibility. We have experimentally tested all the above predictions with an optical setup that we describe in what follows.

Figure 2 shows our experimental setup. Light source is a HeNe laser that delivers a horizontally polarized state $|H\rangle$. After having been submitted to a half-wave plate $H(\alpha)$, state $|H\rangle$ is transformed into $\cos(2\alpha)|H\rangle + \sin(2\alpha)|V\rangle$. A beam displacer (BD) splits the beam into an "up" beam that is horizontally polarized and a "down" beam that is vertically polarized. These two states are simultaneously measured after having been acted upon by polarization changing devices. Due to the relative polarization weights carried by these "up" and "down" components, measurement results correspond to those of the mixed polarization-state

$$\rho_M^{\text{BD}} = \cos^2(2\alpha)|H\rangle\langle H| + \sin^2(2\alpha)|V\rangle\langle V|$$
$$= \frac{1+P}{2}|H\rangle\langle H| + \frac{1-P}{2}|V\rangle\langle V|$$
$$= \frac{1}{2}(\sigma_0 + P\sigma_1), \qquad (11)$$

where $P = \cos(4\alpha)$. With a half-wave plate and a quarter-wave plate in the configuration $H(\pi/8 - \phi/2)Q(0)$, we transform ρ_M^{BD} into the state

$$\rho_M^{\text{in}} = \frac{1 + P\sin\phi}{2}|H\rangle\langle H| - \frac{iP\cos\phi}{2}(|H\rangle\langle V| - |V\rangle\langle H|)$$
$$+ \frac{1 - P\sin\phi}{2}|V\rangle\langle V|$$
$$= \frac{1}{2}(\sigma_0 + P\sin\phi\,\sigma_1 + P\cos\phi\,\sigma_3). \qquad (12)$$

As for the unitary $U_2^\dagger U_1$, setting $U_1 = H(\gamma/8)$ and $U_2 = H(-\gamma/8)$, we get

$$U \equiv U_2^\dagger U_1 = \cos(\gamma/2)\sigma_0 + i\sin(\gamma/2)\sigma_3, \qquad (13)$$

so that U has rotation axis $\hat{n} = (0, 0, 1)$. Notice that we use the optics convention: the diagonal Pauli matrix is $\sigma_1 = |H\rangle\langle H| - |V\rangle\langle V|$, so that linearly polarized states lie on the equator of the Poincaré sphere. The Stokes vector that belongs to ρ_M^{in} is $\vec{S}^{\text{in}} = \text{Tr}(\rho_M^{\text{in}}\vec{\sigma}) = (P\sin\phi, 0, P\cos\phi)$. We can then tune the angle ϕ that $\vec{S}^{\text{in}}$ makes with $\hat{n}$ by means of the aforementioned configuration $H(\pi/8 - \phi/2)Q(0)$.

The intensity at the output of the interferometer is given by Eq. (3). The phase-shift δ is proportional to the voltage applied to a piezoelectric transducer (PZT). By performing intensity measurements, we obtain the visibility V, as defined in Eq. (4). Similarly, by performing polarization tomography we obtain the Stokes vector $\vec{S}_k^{\text{out}}$ that is associated to path k, whereby the other path is blocked. Equation (6) then gives D.

In our experiments, we first kept $\phi = \pi/2$ fixed and chose different values of $P \leq 1$ while changing γ. Our results are shown in Fig. 3. As previously noted, when $P = 0$, $D = 0$, so that in this case the variation of V arises from its dependence on γ and not from a complementary interplay between V and D. This has been confirmed by our results shown in Fig. 3, left upper panel. In the general case, the interplay between
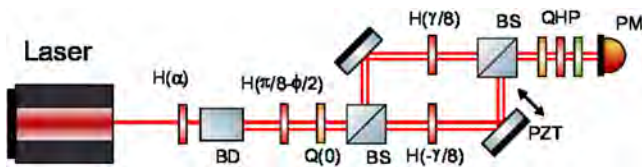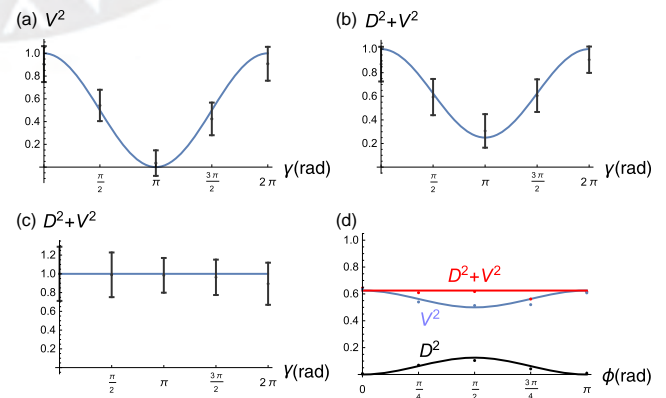

Fig. 2. All-optical setup, appropriate to manipulate a bipartite, path-polarization state. The polarization state serves as a marker of the two-path interferometer. Polarization transformations $H(\pm\gamma/8)$ act as which-path markers. Visibility and distinguishability can be determined by intensity measurements and polarization tomography. BD, beam-displacer; BS, beam-splitter; Q/H, quarter/half-wave plate; P, polarizer; PM, power meter; PZT, piezo-transducer.

Fig. 3. Experimental results for a fixed value of $\phi = \pi/2$ and three values of P. The three cases are: (a) $P = 0 = D$, (b) $P = 0.5$, and (c) $P = 1$. In case (d) $P = 0.5$ and $\gamma = \pi/2$, while $0 \leq \phi \leq \pi$ (in this case, error bars are smaller than symbols).

V and D reflects both complementarity and the action of the polarization-unitary. The case shown in Fig. 3, left bottom panel, corresponds to a fully polarized state: $P = 1$. While in the case $P = 0$ we would expect the unitary to be ineffective, in the case $P = 1$ we would expect the strongest manifestations of the unitary. Our results prove wrong these expectations. We have already commented on this point regarding the case $P = 0$. Now we see that the case $P = 1$ runs also somewhat counter-intuitively. Indeed, according to Eq. (10), if $P = 1$, then $D^2 + V^2 = 1$, irrespective of the action of the unitary. That is, the unitary becomes ineffective precisely when we could have expected it to be most effective, and vice versa. Intermediate cases, e.g., $P = 0.5$, let us see in full the effects captured by the general relationship that is given by Eq. (10) (see Fig. 3, right upper panel). Furthermore, we could also separately test D and V in terms of their dependence on ϕ [see Eqs. (8) and (9)]. To this end, we fixed $\gamma = \pi/2$ and $P = 0.5$ while changing the phase ϕ in the initial Stokes vector. The corresponding results are shown in Fig. 3, right bottom panel. They illustrate how in this case variations of V and D compensate each other so as to maintain $D^2 + V^2$ constant. Error bars in this case are much smaller than that in the previous cases. Such an accuracy level required a lengthy and painstaking procedure to sufficiently reduce the uncertainty of intensity measurements, our dominant error source. This was necessary, because otherwise error bars would intersect the theoretical curves of $D^2 + V^2$ and V^2. In the other cases [Figs. 3(a)–3(c)] the accuracy of our measurements was enough to show agreement between theory and experiment.

All the experimental results are in good agreement with our theoretical predictions. We have thus exhibited the roles played by the various features entering the generalized PCT given by Eq. (10). As we have seen, by taking $\gamma = \pi$, we recover the original form of the PCT: $V^2 + D^2 = P^2$. Thus, our results provide an additional experimental display of the PCT.

We have experimentally displayed, in a classical framework, the complementarity relation between visibility and distinguishability. Similar results should be expected in a quantum framework, because the involved degrees of freedom can be ascribed to both quantum and classical systems. Indeed, the dual nature of some physical phenomena resides in the involved degrees of freedom rather than in their quantum or classical nature. This suggests the possibility of parallel developments towards the exploitation of properties such as coherence, entanglement, etc., that may be used to accomplish various tasks [20–22]. However, an appropriate bridge between communities working in quantum and classical optics is still lacking. For instance, a forerunner of the PCT in its version involving concurrence was proposed some years ago [23]. It came mathematically very close to said version of the PCT, but its physical content markedly differed from the latter. A profitable dialog between the aforementioned communities is thus largely missing.

The extended version of the PCT that we have addressed in this work brings into play some features that the original version left untouched. The so-called marker system—in our case the polarization degree of freedom—can have unitary transformations that are capable of leaving their own imprint in the interplay between visibility and distinguishability associated with it. At least one of these measures of the wave-like and particle-like (or ray-like) nature of the studied phenomenon may survive the disappearance of the marker. As we have seen, when the degree of polarization vanishes, while distinguishability vanishes as well, visibility may keep changing. Changes are ruled in this case by the applied unitary. In contrast, when the degree of polarization attains its maximum value, then the applied unitary does not manifest itself in the interplay between visibility and distinguishability. Our approach allowed us to separately address visibility and distinguishability, thereby exhibiting how they depend on both the marker system and its unitary evolution. We believe that there is still much to be uncovered in relation to effects that show up in connection to hidden and exposed coherences in multipartite systems. The present work has brought just a few aspects of a promising area of research to light.

REFERENCES

1. J. H. Eberly, X.-F. Qian, and A. N. Vamivakas, Optica **4**, 1113 (2017).
2. X.-F. Qian, T. Malhotra, A. N. Vamivakas, and J. H. Eberly, Phys. Rev. Lett. **117**, 153901 (2016).
3. X.-F. Qian, A. N. Vamivakas, and J. H. Eberly, Optica **5**, 942 (2018).
4. G. Jaeger, A. Shimony, and L. Vaidman, Phys. Rev. A **51**, 54 (1995).
5. B.-G. Englert, Phys. Rev. Lett. **77**, 2154 (1996).
6. B.-G. Englert, Z. Naturforsch. **54**, 11 (1999).
7. A. Luis, Opt. Commun. **282**, 3665 (2009).
8. X.-F. Qian and J. H. Eberly, Opt. Lett. **36**, 4110 (2011).
9. X.-F. Qian, B. Little, J. C. Howell, and J. H. Eberly, Optica **2**, 611 (2015).
10. B. Stoklasa, L. Motka, J. Rehacek, Z. Hradil, L. L. Sánchez-Soto, and G. S. Agarwal, New J. Phys. **17**, 113046 (2015).
11. A. Aiello, F. Töppel, C. Marquardt, E. Giacobino, and G. Leuchs, New J. Phys. **17**, 043024 (2015).
12. M. McLaren, T. Konrad, and A. Forbes, Phys. Rev. A **92**, 023833 (2015).
13. J. H. Eberly, Contemp. Phys. **56**, 407 (2015).
14. J. H. Eberly, X.-F. Qian, A. Al Qasimi, H. Ali, M. A. Alonso, R. Gutiérrez-Cuevas, B. J. Little, J. C. Howell, T. Malhotra, and A. N. Vamivakas, Phys. Scr. **91**, 063003 (2016).
15. J. H. Eberly, Laser Phys. **26**, 084004 (2016).
16. N. Sandeau, H. Akhouayri, A. Matzkin, and T. Durt, Phys. Rev. A **93**, 053829 (2016).
17. B.-G. Englert, C. Kurtsiefer, and H. Weinfurter, Phys. Rev. A **63**, 032303 (2001).
18. D. Barberena, O. Ortíz, Y. Yugra, R. Caballero, and F. De Zela, Phys. Rev. A **93**, 013805 (2016).
19. F. De Zela, Optica **5**, 243 (2018).
20. S. M. H. Rafsanjani, M. Mirhosseini, O. S. Magaña-Loaiza, and R. W. Boyd, Phys. Rev. A **92**, 023827 (2015).
21. B. Pinheiro da Silva, M. Astigarreta Leal, C. E. R. Souza, E. F. Galvão, and A. Z. Khoury, J. Phys. B **49**, 055501 (2016).
22. E. Otte, C. Rosales-Guzmán, B. Ndagano, C. Denz, and A. Forbes, Light: Sci. Appl. **7**, 18009 (2018).
23. M. Jakob and J. A. Bergou, Opt. Commun. **283**, 827 (2010).

Experimental display of the extented polarization coherence theorem

Fabio Joel Auccapuclla Quispe

Universidad Católica del Perú

fjauccapuclla@pucp.edu.pe

October 8, 2019

Table of contents

Introduction

Duality and entanglement:

- In 2017, Eberly and coworkers derived the polarization coherence theorem (PCT) [1]

$$V^2 + D^2 = P^2 \tag{1}$$

- Previous work, in a strictly quantum context, constrained V and D by inequalities such as [2-4]

$$V^2 + D^2 \leq 1 \tag{2}$$

- In 2018, F. de Zela found a extension of the PCT [5]

$$V^2 + D^2 = \cos^2 \frac{\gamma}{2} + P^2 \sin^2 \frac{\gamma}{2} \tag{3}$$

Physical Framework
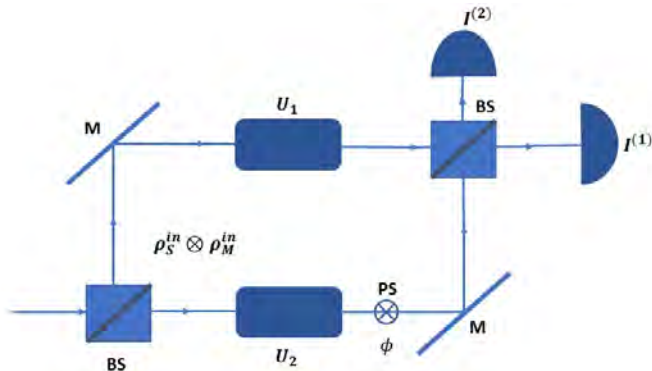
Figure: Mach-Zender interferometer. A product-state system-marker is submitted to unitaries U_1 and U_2 that act on the marker alone. BS, beam-splitter; PS, phase-shifter.

Physical Framework

A two-arm interferometric setup with transformation (U_1 and U_2) in each arm. These apply to an "internal" DOF, e.g., electron's spin or photon's polarization. Both DOFs can be represented in a two-dimensional Hilbert space. The internal DOF serves as a path marker.

Note: More effective less visible is the interferogram and the marker then more distinguishable.

Theoretical Background

- The system S is in the pure state $|\psi_S^{in}\rangle = \alpha |1\rangle + \beta |2\rangle$ then

$$\rho_S^{in} = |\psi_S^{in}\rangle \langle \psi_S^{in}| = |\alpha|^2 \, \sigma^\dagger \sigma + |\beta|^2 \, \sigma \sigma^\dagger + \alpha \beta^* \sigma^\dagger + \alpha^* \beta \sigma \qquad (4)$$

  with $\sigma = |2\rangle \langle 1|$ and $\sigma^\dagger = |1\rangle \langle 2|$

- The marker M is in the mixed state $\rho_M^{(0)}$. It can be represented as a mixed state using Pauli matrices (σ_0 and $\vec{\sigma}$) and the Stokes vector ($\vec{S}$)

$$\rho_M^{in} = \frac{1}{2}(\sigma_0 + \vec{S}^{in} \cdot \vec{\sigma}) \qquad (5)$$

The whole system will be submitted through the no-local transformation U_{SM}

$$U_{SM} = \sigma^\dagger \sigma U_1 + \sigma \sigma^\dagger U_2 e^{i\phi} \tag{6}$$

where U_i is a polarization-unitary transformation in the arm i. Then, we have the system in the state

$$\rho_{SM} = U_{SM}(\rho_S^{in} \otimes \rho_U^{in})U_{SM}^\dagger \tag{7}$$

Path-System

In order to analyze the Path-System, we use $\rho_S = Tr_M(\rho_{SM})$. The intensity at one output of the interferometer

$$I = \frac{1}{2}\left\{|\alpha|^2 + |\beta|^2 + 2Re[\alpha^*\beta\, Tr_M(U_1\rho_M^{in}U_2^\dagger e^{i\delta})]\right\} \tag{8}$$

Then, the visibility is defined as

$$V = \frac{I_{max} - I_{min}}{I_{max} + I_{min}} = \left| Tr_M(U_1\rho_M^{in}U_2^\dagger)\right| = \left| Tr_M(U\rho_M^{in})\right| \tag{9}$$

with $U = U_2^\dagger U_1$, it can be seen as a relative unitary transformation.

Marker-System

The Marker-System is in the following state

$$\rho_M = Tr_S(\rho_{SM}) = |\alpha|^2 \, \rho_M^{(1)} + |\beta|^2 \, \rho_M^{(2)} \tag{10}$$

where $\rho_M^{(k)} = U_k \rho_M^{in} U_k^\dagger$ ($k = 1, 2$). In equation (10), ρ_M is a weighted sum of $\rho_M^{(1)}$ and $\rho_M^{(2)}$. Also, equation (10) suggests us to define the distinguishability between the two paths as

$$
\begin{aligned}
D &= \tfrac{1}{2} Tr \left| \rho_M^{(1)} - \rho_M^{(2)} \right| \\
&= \tfrac{1}{2} Tr \left| U_1 \rho_M^{in} U_1^\dagger - U_2 \rho_M^{in} U_2^\dagger \right| \\
&= \tfrac{1}{2} \left| \vec{S}_1^{out} - \vec{S}_2^{out} \right|
\end{aligned}
\tag{11}
$$

where $|A| = \sqrt{A^\dagger A}$, A linear operator and $\vec{S}_k^{out}$ Stokes vector associated to $\rho_k^{(k)}$.

Marker-System

Writing $\vec{S}_k^{out} = \mathcal{R}_k \vec{S}^{in}$, $\mathcal{R}_k$ is a 3D-rotation that is associated to U_k. Distinguishability

$$D = \frac{1}{2} \left| \mathcal{R}_1 \vec{S}^{in} - \mathcal{R}_2 \vec{S}^{in} \right| = \frac{1}{2} \left| \mathcal{R}_2^{-1} \mathcal{R}_1 \vec{S}^{in} - \vec{S}^{in} \right| \qquad (12)$$

All the calculation lies in the rotation $\mathcal{R}_2^{-1} \mathcal{R}_1$. This rotation can be parameterized by a rotation angle γ and a rotation axis $\hat{n}$. $\mathcal{R}_2^{-1} \mathcal{R}_1$ has a unitary transformation associated $U_2^\dagger U_1$, whose expression is

$$U = U_2^\dagger U_1 = \cos\left(\frac{\gamma}{2}\right) \sigma_0 + i \sin\left(\frac{\gamma}{2}\right) \hat{n} \cdot \vec{\sigma}_0 \qquad (13)$$

Marker-System

Using this parameterization, we compute the following relations

$$D^2 = P^2 \sin^2(\phi) \sin^2\left(\frac{\gamma}{2}\right) \tag{14}$$

$$V^2 = \cos^2\left(\frac{\gamma}{2}\right) + P^2 \cos^2(\phi) \sin^2\left(\frac{\gamma}{2}\right) \tag{15}$$

where ϕ is the angle between $\hat{n}$ and $\vec{S}^{in}$.
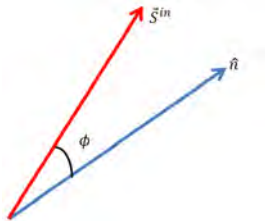
Figure: ϕ: Angle between $\vec{S}^{in}$ and $\hat{n}$

Marker-System

Adding (14) and (15)

$$D^2 + V^2 = \cos^2\left(\frac{\gamma}{2}\right) + P^2 \sin^2\left(\frac{\gamma}{2}\right) \tag{16}$$

- Since $P^2 \leq 1$ we derive relations [2-4]

$$D^2 + V^2 \leq 1 \tag{17}$$

- If the Marker system is in pure state $(P = 1)$ we derive Englert relation [3]

$$D^2 + V^2 = 1 \tag{18}$$

- If we fix $\gamma = \pi$ we derivate Eberly-Qian-Vamivakas relation [1]

$$D^2 + V^2 = P^2 \tag{19}$$
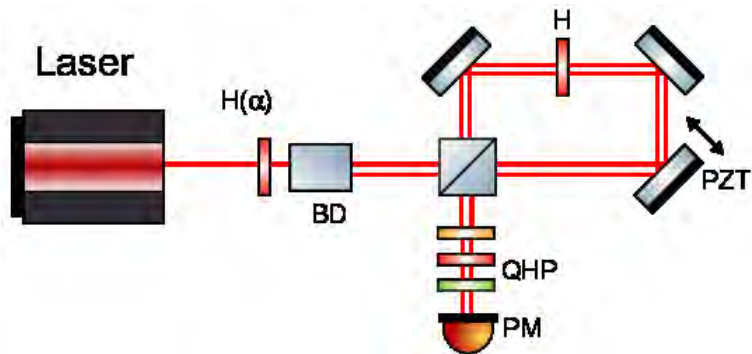
Figure: Experimental setup and detection

Using a Half Wave Plate followed by a Beam Displacer we get the following mixed state

$$\rho_M^{BD} = \cos^2(2\alpha) \left| H \right\rangle \left\langle H \right| + \sin^2(2\alpha) \left| V \right\rangle \left\langle V \right|$$
$$= \frac{1}{2}(\sigma_0 + P\sigma_1) \tag{20}$$

where $P = \cos(4\alpha)$.
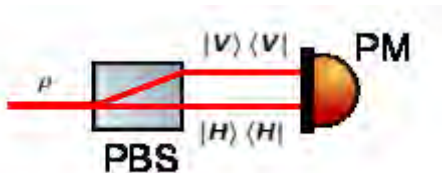
Figure: Polarization Beam Displacer

We have $\rho_M^{in} = \rho_M^{BD}$, $U_1 = H(\gamma/8)$ and $U_2 = H(-\gamma/8)$. Then,

$$U = U_2^\dagger U_1 = \cos(\gamma/2)\sigma_0 + i\sin(\gamma/2)\sigma_3 \qquad (21)$$

so U has a rotation axis $\hat{n} = (0, 0, 1)$. Since, the Stokes vector of ρ_M^{in} is
$\vec{S}^{in} = (1, 0, 0)$ $\phi = \frac{\pi}{2}$ fixed.

- To measure V we changed the phase-shift δ using the PZT and
  recorded intensity.
- To measure D we performed polarization tomography to obtain $\vec{S}_k^{out}$
  associated to path k, whereby the other path is blocked.

Results
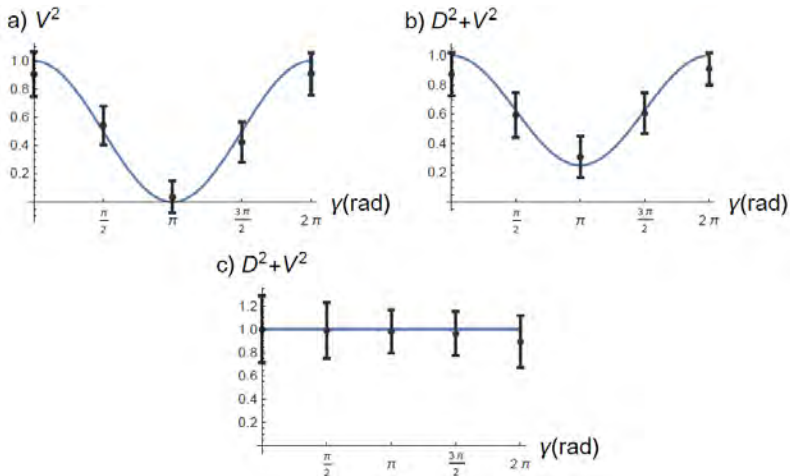
Figure: Experimentals results for a fixed value of $\phi = \pi/2$ and three values of P. The three cases are: (a)P=0=D, (b)P=0.5, and (c)P=1.

Mach-Zender Interferometer
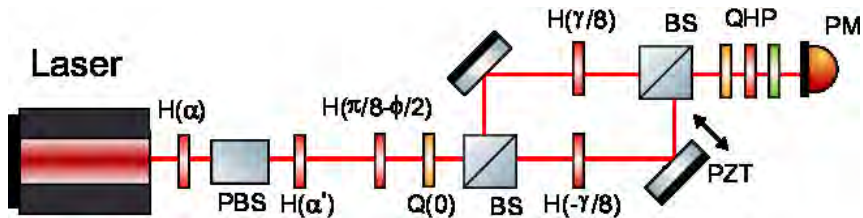
Figure: Experimental setup and detection

Phase's calculations

Actually, we just have one level here. To simulate the mixed state with degree of Polarization (P)

$$\rho_M^{mix} = \frac{1+P}{2}\left|h\right\rangle\left\langle h\right| + \frac{1-P}{2}\left|v\right\rangle\left\langle v\right| \tag{22}$$

we express ρ_M^{in} as $\rho_{hh} + \rho_{vv}$. Both of them are generated by the following set of angles in a Half-Wave Plate

$$
\begin{aligned}
\alpha &= \frac{ArcCos(P)}{4} \ \ \& \ \ \alpha' = 0 &&\longrightarrow \rho_{hh} \\
\alpha &= \frac{\pi}{4} - \frac{ArcCos(P)}{4} \ \ \& \ \ \alpha' = \frac{\pi}{4} &&\longrightarrow \rho_{vv}.
\end{aligned}
\tag{23}
$$

As it was mentioned ρ_{hh} and ρ_{vv} evolve independently from each other and they do not exist at the same time. In fact, each one is not a density matrix by a constant multiplication factor. Anyway, both of them evolve using a $H(\pi/8 - \phi/2)$ followed by a $Q(0)$

$$\rho'_{hh} = \frac{1+P}{2} \begin{bmatrix} \cos^2(\frac{\pi}{4} - \frac{\phi}{2}) & -i\cos\frac{\phi}{2} \\ i\cos\frac{\phi}{2} & \sin^2(\frac{\pi}{4} - \frac{\phi}{2}) \end{bmatrix} \tag{24}$$

$$\rho'_{vv} = \frac{1-P}{2} \begin{bmatrix} \sin^2(\frac{\pi}{4} - \frac{\phi}{2}) & i\cos\frac{\phi}{2} \\ -i\cos\frac{\phi}{2} & \cos^2(\frac{\pi}{4} - \frac{\phi}{2}) \end{bmatrix} \tag{25}$$

Each one has an I^{out}, replacing (24) and (25) in (8)

$$I_{hh} = \frac{1+P}{2}(1 + \cos\frac{\gamma}{2}\cos\delta - \sin\frac{\gamma}{2}\cos\delta\cos\phi) \qquad (26)$$

$$I_{vv} = \frac{1-P}{2}(1 + \cos\frac{\gamma}{2}\cos\delta + \sin\frac{\gamma}{2}\cos\delta\cos\phi) \qquad (27)$$
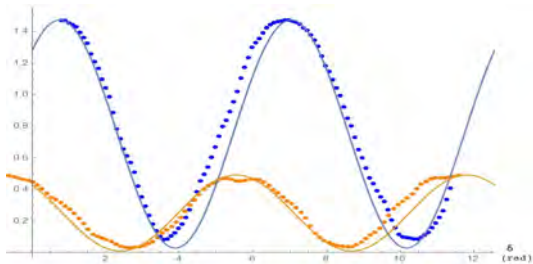

Figure: Values of I^{out} measured and post-processed data for $P = 0.5$, $\gamma = \pi/2$ and $\phi = \pi/4$. Blue points and orange points correspond I_{hh} and I_{vv}, respectively.

Measurements

What is important for us is $\rho_M^{in} = \rho'_{hh} + \rho'_{vv}$

$$\rho_M^{in} = \frac{1}{2}[\sigma_0 + P\sin(\phi)\sigma1 + P\cos(\phi)\sigma_3] \qquad (28)$$

thus $\vec{S}^{in} = P(\sin\phi, 0, \cos\phi)$. We used the same transformations U with rotation axis $\hat{n} = (0, 0, 1)$. We had complete control over ϕ.

- After processing I_{hh} and I_{vv} we calculate V.
- To calculate D we measure each component's polarization, i.e. h,v,d,a,r and l, for ρ'_{hh} and ρ'_{vv}. Then, we just add $I_{hh,k}^{h}$ and $I_{vv,k}^{h}$ to get I_k^h, where $k = 1, 2$ represents path 1 or 2. We repeat the same process for all the components, then we get $\vec{S}_k^{out}$. Do not forget that we blocked one path to measured the other.
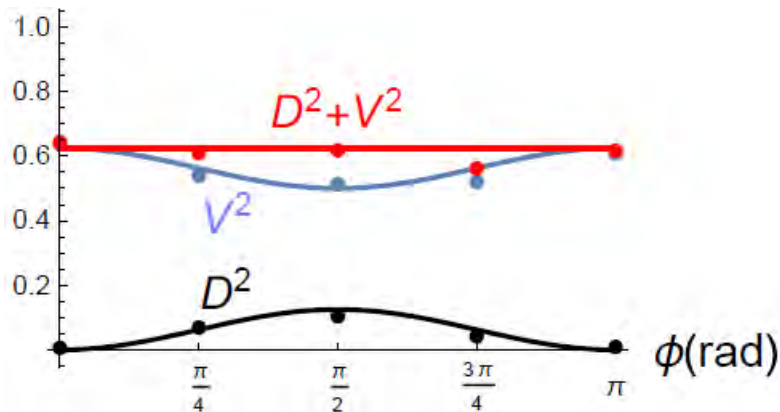
Figure: For fixed values of $P = 0.5$ and $\gamma = \pi/2$, while $0 \leq \phi \geq \pi$

Conclusions

- In a classical framework we experimentally displayed the complementarity relation between visibility and distinguishability.

- We held $\phi = \pi/2$, on the Sagnac interferometer, with different values of P while changing γ. When $P = 0$ and $D = 0$ the variation of V comes about from its dependence on γ and not from a complementary interplay between V and D. In the general case, both complementarity and the action of the polarization-unitary are reflected in the interplay between V and D.

- We tested separately D and V, on the Mach-Zender interferometer, in terms of their dependences on ϕ.

References

1. J. H. Eberly, X.-F. Qian, and A. N. Vamivakas, Optica **4**, 1113 (2017).

2. G. Jaeger, A. Shimony, and L. Vaidman, Phys. Rev. A **51**, 54 (1995).

3. B.-G. Englert, Phys. Rev. Lett. **77**, 2154 (1996).

4. B.-G. Englert, Z. Naturforsch. **54a**, 11 (1999).

5. F. De Zela, Optica **5**, 243 (2018).